Available online at www.sciencedirect.com
SCIENCE DIRECT
Earth and Planetary Science Letters 240 (2005) 790–802
EPSL
www.elsevier.com/locate/epsl

Characteristics and genesis of maghemite in Chinese loess and paleosols: Mechanism for magnetic susceptibility enhancement in paleosols

Tianhu Chen [a,b], Huifang Xu [b,*], Qiaoqin Xie [a], Jun Chen [c], Junfeng Ji [c], Huayu Lu [d]

[a] School of Natural Resources and Environment, Hefei University of Technology, Hefei, Anhui 230009, China
[b] Department of Geology and Geophysics, University of Wisconsin, Madison, WI 53706, USA
[c] Department of Earth Sciences, Nanjing University, Nanjing 210093, China
[d] State Key Laboratory of Loess and Quaternary Geology, Institute of Earth Environment, Chinese Academy of Sciences, Xi'an, Shaanxi 710075, China

Received 5 March 2005; received in revised form 29 June 2005; accepted 19 September 2005
Available online 8 November 2005
Editor: E. Boyle

Abstract

Morphological characteristics and microstructures of magnetic minerals extracted from Chinese loess and paleosols were investigated using powder X-ray diffraction (XRD) and high-resolution transmission electron microscopy (HRTEM). Our results indicate that maghemite in loess–paleosol sequences was transformed from magnetite through oxidation of magnetite. Maghemite transformed from eolian magnetite during chemical weathering has low-angle grain boundaries among maghemite nano-crystals. Some nano-crystalline maghemites with nanoporous texture resulted from microbe-induced precipitation of magnetite or transformation of poorly crystalline ferric Fe (oxy)hydroxides in presence of Fe-reducing bacteria. Aggregates of euhedral maghemite nano-crystals were transformed from magnetite magnetosomes. Both microbe-induced nanoporous magnetite and microbe-produced magnetite magnetosomes are directly related to microbial activities and pedogenesis of the paleosols. It is proposed that the formation of nano-crystalline maghemite with superparamagnetic property in paleosol results in the enhancement of magnetic susceptibility, although the total amount (weight percent) of magnetic minerals in both paleosol and loess units is similar. Our results also show that nano-crystalline and nanoporous magnetite grains prefer to transform into maghemite in semi-arid soil environments instead of hematite, although hematite is a thermodynamically stable phase. This result also indicates that a decrease in crystal size will increase stability of maghemite. It is also inferred that surface energy of maghemite is lower than that of hematite.

Keywords: loess; paleosol; maghemite; biogenic magnetite; magnetic susceptibility; Transmission Electron Microscopy (TEM)

1. Introduction

Chinese loess is regarded as one of the best continental record of paleoclimatic and paleoenvironmental changes during the late Cenozoic era. There are numerous papers discussing paleoclimate changes based on magnetic susceptibility variations in the loess–paleosol sequences. The striking correlation between the variations of color and magnetic susceptibility (MS) in Chinese loess–paleosol sequences and the marine oxygen isotope records have shown that the loess and paleosol units formed during glacial and interglacial

* Corresponding author. Tel.: +1 608 265 5887; fax: +1 608 262 0693.
E-mail address: hfxu@geology.wisc.edu (H. Xu).

0012-821X/$ - see front matter © 2005 Elsevier B.V. All rights reserved.
doi:10.1016/j.epsl.2005.09.026

episodes, respectively. The Chinese loess provides a complete record of East Asia paleoclimatic change over 2.5 Ma [1]. The magnetic susceptibility of Quaternary loess can be easily measured and extensively used as proxy for paleoclimate [2–6]. There are several proposed mechanisms for magnetic susceptibility enhancement of the paleosol units, which include chemical weathering [7], magnetite deposition/accumulation [8], natural fire [9], pedogenesis [10,11], magnetotactic bacteria mineralization [12], and inorganic precipitation via iron reduction by iron-reducing bacteria [4]. The changes of color and magnetic susceptibility in loess–paleosol sequences result from changing concentration and composition of iron oxides. Iron oxides and oxyhydroxides including magnetite, goethite, hematite were first identified in loess–paleosol sequences by Heller and Liu [13] using optical microscopy. The existence of maghemite has also been supported by magnetic property and Mossbauer spectroscopy studies. Maghemite is also considered as a major carrier of magnetic susceptibility in loess–paleosol sequences [14–20]. Because iron oxides are usually very fine grains with low crystallinity and low concentration in loess, traditional mineralogy analysis methods are not sensitive enough to identify them. Maher [4] and Vandenberghe et al. [21] used magnetic extraction methods to isolate strong magnetic iron oxides from soils. However, it is difficult to identify the mineral composition of magnetically extracted fractions because both magnetite and maghemite are very similar in their structures and chemical compositions [22–24]. The magnetic minerals in loess–paleosol sequences were identified by indirect methods, such as magnetic property, Mössbauer spectroscopy measurements, or differential extraction. It was considered that there are large amounts of ultra-fine magnetic particles in paleosol units [10,25]. However, the mineral composition of the ultra-fine magnetic particles (i.e., magnetite and/or maghemite) and their formation process were not well understood. Although it was considered that ultra-fine maghemite in the loess and paleosols is of authigenic origin and formed during pedogenesis, there are no direct observations of the maghemite. It is very difficult to understand formation of the maghemite and the mechanism for magnetic susceptibility enhancement in paleosol units without knowing details of this nanometer-scale maghemite.

By analyzing magnetic minerals using transmission electron microscopy (TEM), Maher et al. have suggested that entirely euhedral and ultra-fine magnetic particles were attributed to magnetotactic bacteria biomineralization, and all the sub-micrometer particles with nanoporous structure were formed through inorganic precipitation by iron-reducing bacteria [4]. TEM that can study mineral structures, microstructures, and compositions at the atomic scale is a very useful tool for studying textures and mineral reactions of the fine-grained Fe-oxide minerals [27–30]. In this paper, we use this method to identify maghemite and magnetite minerals extracted from the loess–paleosol units, although differential chemical extraction of Fe method (citrate–bicarbonate–dithionite treatment) was also used to distinguish magnetite and maghemite [15,18]. It was expected that the study at the nanometer scale will help us to understand mineral characteristics, mineral formation mechanisms, and magnetic susceptibility enhancement in paloesol units, which will support studies in the areas of magnetic stratigraphy, geochemical processes of pedogenesis, and paleoclimate reconstruction in the loess–paleosol sequences. The study will also help us to understand role of ferric Fe reduction bacteria in the formation of magnetite.

2. Sample settings and experimental methods

Our samples were collected from following sites: the classic Luochuan, Huanxian and Xifeng sections. The extracted samples from one loess unit (L1), two paleosol units (S1, S3) and a red clay unit were used for this study.

Magnetic extraction methods were described previously [31,32]: (1) adding 10.0 g of loess sample and a magnetic stir bar covered by Teflon into a 1000-mL beaker; (2) stirring the loess/water suspension with a magnetic stirrer for 2 h at a rate of 100 rpm; (3) using non-magnetic tweezers to pick up the magnetic bar after stopping; the magnetic bar is covered a layer of dark and dark-brown powers; gently wash the bar three times with distilled water to remove clay minerals on surface; (4) repeating the above processes until the magnetic bar does not take up any magnetic minerals from the beaker; the extracted minerals were used for scanning electron microscope (SEM), TEM and XRD analyses.

TEM investigation was carried out in the Department of Earth and Planetary Science, the University of New Mexico, USA. A JEOL 2010 HRTEM with an attached Oxford Instruments X-ray EDS system was used for TEM imaging and selected-area electron diffraction study [33]. A JEOL 2010F FASTEM with attached Oxford Instruments X-ray EDS system and Gatan Imaging Filtering (GIF) system was used for collecting electron energy-loss spectra that can identify oxidation states of transitional metals [34,35]. The XRD analyses were carried out in the Structural Anal-

ysis Center, Hefei University of Technology with a D/max-RB type power diffractometer (Cu-target, 40 kV, 100 mA, scan rate 2°/min). The SEM analyses were carried out in the Structural Analysis Center of the University of Science and Technology of China with a HITACHI X-650 SEM.

3. Identification and characteristics of maghemite

3.1. XRD identification of maghemite

Although the color of maghemite is the difference from that of magnetite, the crystal structure of maghemite (γ-Fe_2O_3) is similar to that of magnetite (Fe_3O_4). The main structural and chemical difference between maghemite and magnetite is the existence of vacancies in maghemite, which lowers the symmetry of maghemite (primitive Bravais lattice) with respect to magnetite (face-centered Bravais lattice). Further ordering of the vacancies results in a tetragonal supperlattice structure with $c=3a$ [53–57]. In general, solid-state oxidation of magnetite may result in maghemite formation. Because magnetite and maghemite are very similar in their structures and their XRD patterns, diffraction peaks from magnetite nearly overlap with those from maghemite. Unit cell parameters for magnetite- and maghemite-based cubic setting are 0.840 nm and 0.835 nm, respectively. A slight difference in unit cell parameters results in a slight shift of all peaks from maghemite towards higher angles with respect to the peaks from magnetite (Fig. 1). When magnetite and maghemite coexist together, diffraction peak intensity and peak shape will change as their proportions change. In general, it is difficult to identify them by using powder XRD analysis alone.

There are various minerals in loess–paleosol sequences, especially, quartz, calcite, and clay minerals. Concentration of magnetite and maghemite in loess–paleosol sequences is too low to be directly detected by XRD analysis based on counts of faint diffraction peaks from bulk samples. Wet magnetic extraction is an efficient method to enrich ferromagnetic minerals from the loess–paleosol samples for quantitative study of the magnetic minerals. The XRD patterns of magnetically extracted samples are displayed in Fig. 2. The diffraction peaks corresponding to magnetite and hematite are obvious. A majority of the extracted fractions are iron oxides with small amounts of quartz also present. Therefore, relatively pure iron oxide mixtures with low concentration of impurities can be obtained through the magnetic extraction. Fig. 3 that displays enlarged areas from Fig. 2 clearly shows that the diffraction peaks of magnetite/maghemite, such as 220, 511, and 440, obviously shift towards higher angles with respect to those from pure magnetite. These peaks are strong diffraction peaks from magnetite and maghemite. Contribution from hematite at these positions is very weak. Meanwhile, the 104 peak ($d=2.69$ Å) of hematite in all samples does not shift, which indicates that peak shifts are caused by the presence of both magnetite and maghemite in the studied samples. The peak shifts are not from instrumental error. Therefore, the shifts of 220,

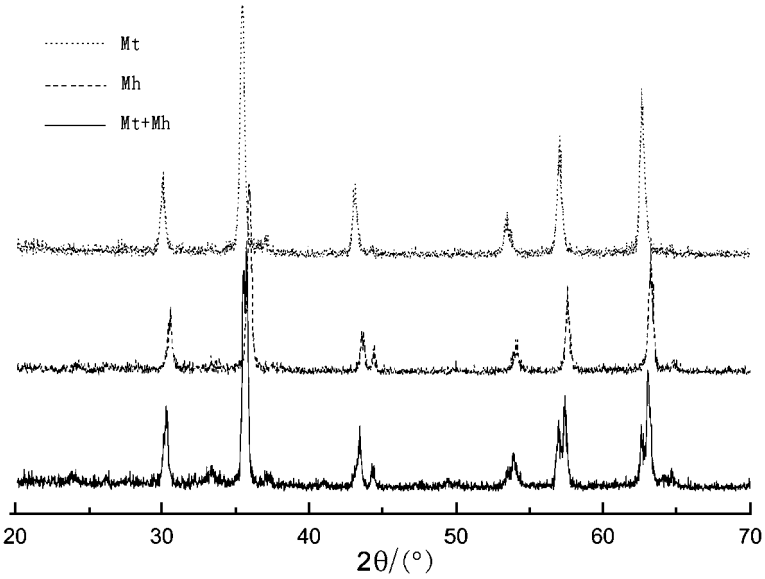

Fig. 1. Powder XRD patterns of synthetic magnetite and maghemite. Mt: maghemite (top); Mh: maghemite (middle); Mt+Mh: 1:1 mixtures of magnetite and maghemite (bottom).

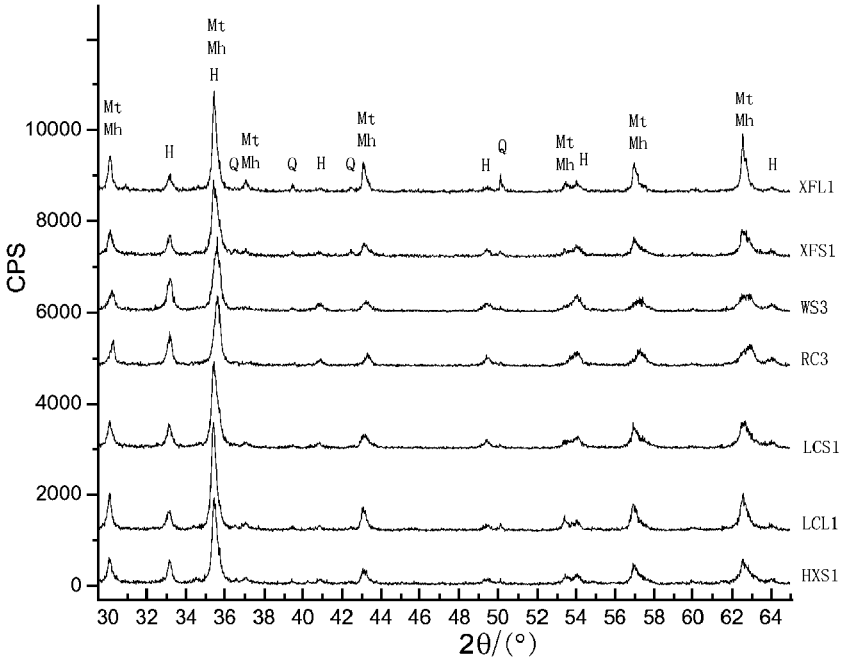

Fig. 2. Powder XRD patterns of magnetically extracted fractions from the loess–paleosol sequences. H–hematite; Mt–magnetite; Mh–maghemite; Q–quartz; XFL1–Xifeng loess, unit L1; XF13–Xifeng paleosol, unit S1; WS3–Wucheng paleosol, unit S3; RC–red clay layer; LCL1–Luochuan loess, unit L1; HXS1–Huanxian paleosol, unit S1.

511, 440 peaks of the magnetic samples indicate that there are some amounts of maghemite in the extracted samples. Compared with the samples from the loess unit, diffraction peaks corresponding to magnetite from the paleosol are weaker, broader, and less symmetrical. Our further TEM study in the next section will discuss evidence that these features result from the formation of nanometer-scale maghemite and ox-

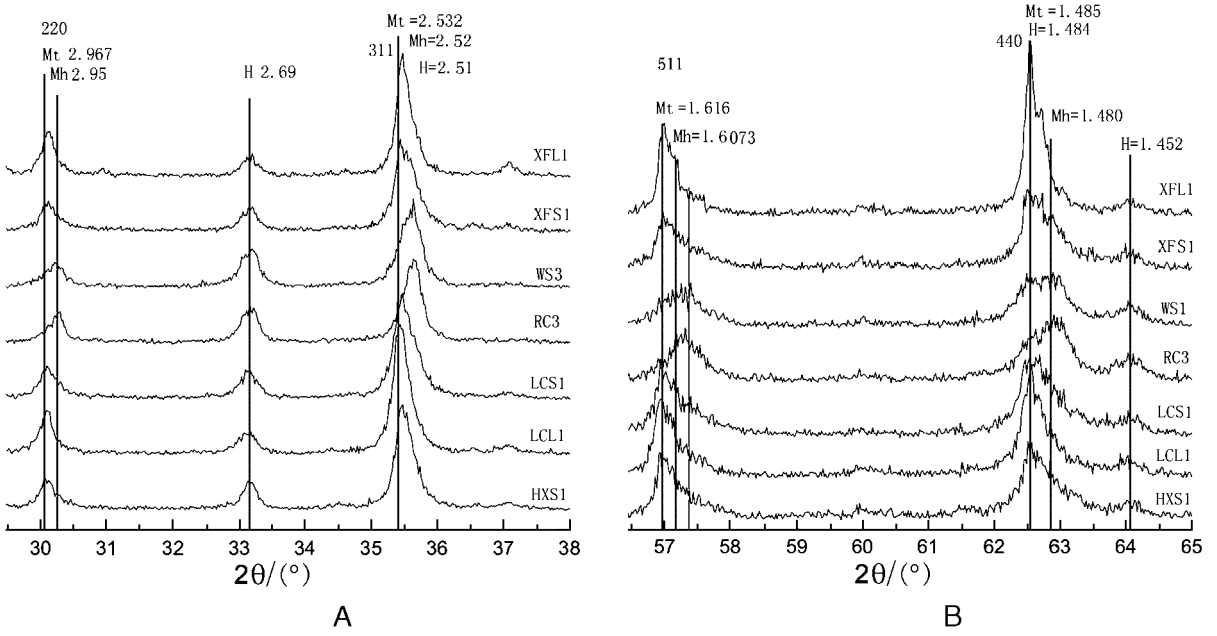

Fig. 3. Powder XRD patterns of magnetically extracted minerals from the loess–palaeosol sequences. H–hematite; Mt–magnetite; Mh–maghemite; XFL1–Xifeng loess, unit L1; XF13–Xifeng palaeosol, unit S1; WS3–Wucheng paleosol, unit S3; RC–red clay layer; LCL1–Luochuan loess unit, L1; HXS1–Huanxian paleosol, unit S1.

idative transformation from magnetite to maghemite nano-crystals.

3.2. TEM identification and characteristics of maghemite

The magnetically extracted samples were directly deposited onto holey carbon-coated Cu grids that were used for TEM observations. The main structural difference between magnetite and maghemite is their Bravais lattice. Magnetite has a face-centered lattice (F) structure, whereas maghemite has a primitice (P) superlattice structure. Therefore, {110} reflections that are extinct in magnetite will appear in maghemite [36]. If we have [001] zone-axis high-resolution TEM (HRTEM) images from both magnetite and maghemite, the image from maghemite will display 5.9-Å (110) lattice fringes, whereas the image from magnetite will only display 3-Å (220) lattice fringes. Associated techniques of X-ray energy-dispersive spectra collected from a particular area can also help us to differentiate the oxides from silicate minerals. Selected area electron diffraction patterns can help us to differentiate the magnetite and maghemite from other iron oxide minerals. In addition, electron energy-loss spectroscopy will help us to obtain the valence state of Fe. The integrated TEM study is a useful method for investigating the fine-grained magnetite and maghemite. We investigated 15 magnetically extracted samples from loess–paleosol sequences using TEM and associated techniques. The maghemite has the following characteristics according to our TEM observations.

(1) Sub-micrometer-scale and smaller magnetic grains that have morphological characteristics of eolian origin were transformed into maghemite that displays 5.9-Å (110) lattice fringes (Fig. 4). Because the magnetite was completely oxidized into maghemite, the resulting maghemite has small crystalline domains with low-angle boundaries among the maghemite nano-crystals. The arc-like streaking diffraction in its SAED pattern clearly indicates the low-angle grain boundaries in the transformed maghemite (Fig. 4). The angles measured from the SAED pattern are less than 10°.
(2) Sub-micrometer grains from the loess unit that have morphological characteristics of eolian origin, with edges and surfaces transformed into maghemite that displays 5.9-Å (110) lattice fringes. The grains still preserve single-crystal morphology. However, SAED pattern with arc-like streaking diffraction from the grain shows multi-crystal domains with low-angle grain

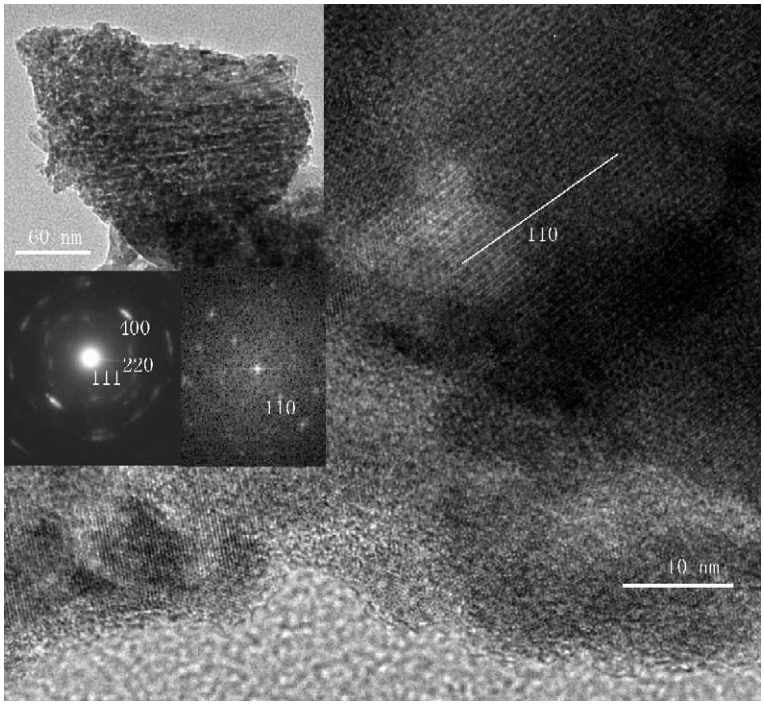

Fig. 4. High-resolution TEM image from an edge of the maghemite grain (inserted, upper-left corner). An SAED pattern from the grain and a [−110] zone-axis Fast Fourier Transform (FFT). The sample is from paleosol S1 unit.

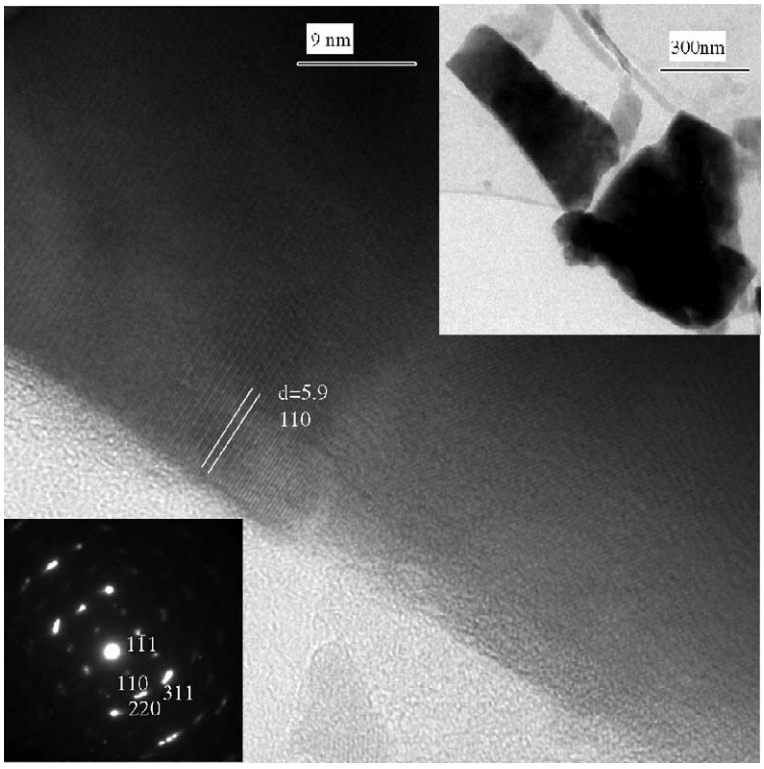

Fig. 5. HRTEM image shows 5.9-Å (110) lattice fringes of maghemite in a local area of an eolian grain. Inserted are low-magnification TEM image (upper-right corner) and SAED pattern (lower-left corner) of a partially oxidized magnetite. This sample is from loess L1 unit.

boundaries (Fig. 5). This kind of texture result from oxidative transformation of magnetite to maghemite. The single-crystal domain size of the maghemite is much smaller than that of the eolian magnetite grain.

(3) Some sub-micrometer grains display nanoporous texture that is composed of nano-crystalline maghemite (Fig. 6). The SAED pattern from one of the grains shows powder diffraction rings. The powder diffraction pattern does not show a 110 diffraction ring because of very weak 110 refraction and highly disordered maghemite structure. Electron energy-loss spectrum from the nanoporous grain shows an L_3

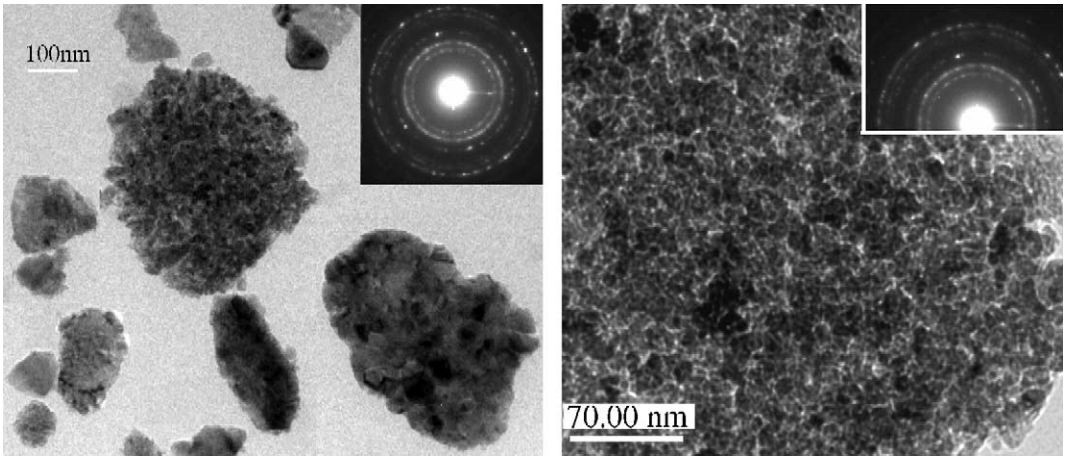

Fig. 6. Bright-field TEM images of the maghemite from a paleosol unit. The right image is an enlarged area of the nanoporous maghemite. Inserted SAED pattern at upper-right corners is from the grain with a nanoporous structure. The first three diffraction rings are 200, 111, and 220 reflections. This sample is from Luochuan paleosol S1 unit.

edge peak at ~710 eV, which indicates the presence of ferric Fe in the structure [35,37]. Such nanoporous structure is composed of randomly oriented maghemite nano-crystals. This sample is from the paleosol S1.

4. Maghemite genesis

Maher et al. [4] suggested that all ferromagnets possessing nanoporous structure were formed from inorganic precipitation via iron reduction by iron-reducing bacteria. Based on our systematic study on magnetically extracted samples using TEM, the ferromagnetic minerals with nanoporous structure are more common in paleosol units than in loess units. It is proposed that such kind of magnetite was induced by microbes in soil environment. Microbes could generate a locally reducing environment that can promote magnetite formation [56,57], which results in the formation of a composite of nano-crystalline magnetite and organic matters produced by microbes.

We consider the nanoporous magnetite that has transformed into maghemite as biogenic magnetite. It is proposed that the nanoporous magnetite grains like that in Fig. 6 were resulted from dissimilatory reduction of ferric Fe and in situ precipitation of magnetite nano-crystals in locally reducing environments. Dissimilatory reduction of ferric Fe is a common reaction in soil environments [56,57]. The other alternative for the nanoporous magnetite formation is the interaction between ferric Fe-reducing bacteria and poorly crystalline ferric Fe (oxy)hydroxide (such as ferryhydrite) through dissolution/re-crystallization process and/or enzyme-mediated reactions between ferryhydrite and microbial reduced ferrous Fe. Such kind of microbe-induced magnetite nano-crystals can precipitate in a system containing bacteria of *Geobacter sulfurreducences* [58]. Poorly crystalline ferric Fe precipitates are very reactive in microbial respiration process [59]. The ferric Fe-reducing bacteria may transform ferryhydrite into magnetite and preserve nanoporous texture. The nanopore areas could be rich in bio-organics. Decomposition of the organics and oxidation of the magnetite at solid state results in the formation of nanoporous maghemite. A nanoporous magnetite from a modern loess on basalt lava in the area of Albuquerque Volcanoes, New Mexico, shows small amounts of P and S besides Fe and O (Fig. 7). A detailed mechanism for the nanoporous magnetite formation in water-unsaturated loess and the role of ferric Fe-reducing bacteria needs to be investigated in the future.

It was also observed that some nanoporous ferromagnetic grains are nano-crystalline maghemite, resulting, at least partially, from magnetite oxidation at solid state. Especially in Fig. 8, a sub-angular ferromagnetic particle connected with a rutile crystal is obviously an eolian magnetite. At present, this grain is a multi-crystal maghemite with nanoporous structure. The SAED pattern from the transformed porous maghemite does not show random orientation of the maghemite nano-crystals. Therefore, not all the nanoporous structures resulted from biologically induced precipitation. The nanoporous maghemite can be formed through the oxidation of magnetite. A majority of magnetic iron oxides in large eolian grains are magnetite. It is difficult for maghemite to precipitate from water solution directly. In general, maghemite is transformed from magnetite through solid-state phase transformation, such as magnetite oxidation, lepidocrocite dehydration at high temperature, or organic-catalyzed goethite dehydration

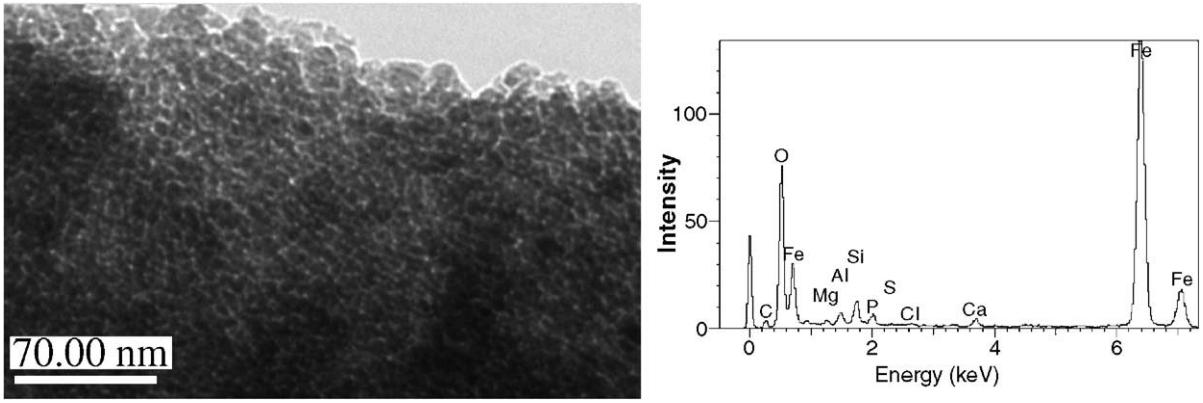

Fig. 7. Left: TEM image shows a nanoporous magnetite from a modern loess in Albuquerque, NM. Right: X-ray energy-dispersive spectrum from area in left image shows Fe and oxygen with small amount of P that may be from bio-organics in the nanopores. The nanometer-scale pores here are worm-hole-like nanopores. Bright areas correspond to low electron density areas of nanopores.

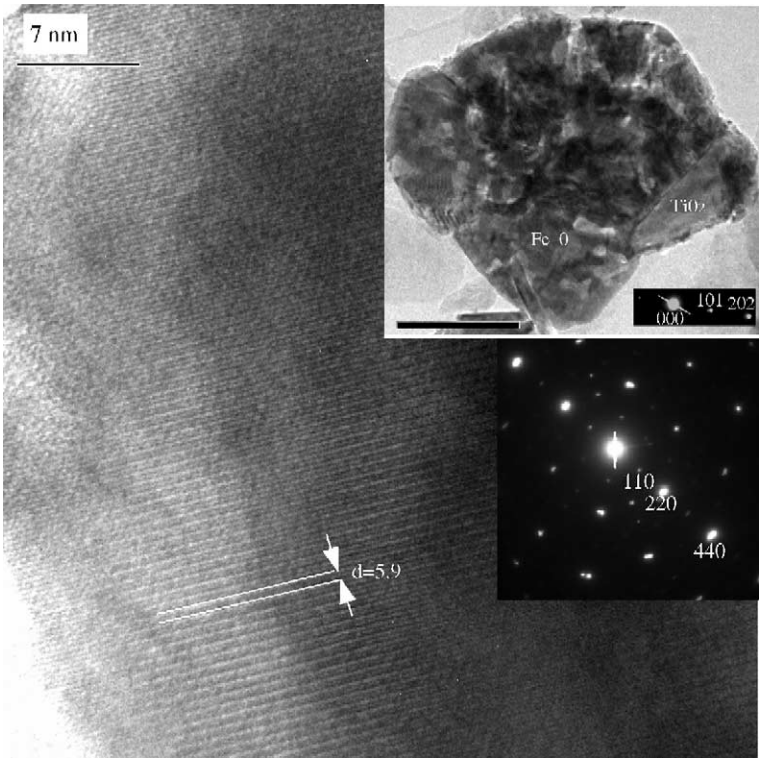

Fig. 8. HRTEM image of an eolian grain that has transformed into maghemite. Its low-magnification TEM image (upper-right corner) shows nanoporous texture and an attached rutile crystal. Its SAED pattern (lower-right corner) shows 110 reflection from maghemite structure. This sample is from paleosol S1 unit.

under surface/soil condition [38,39]. Therefore, abundant magnetite–maghemite complexes in loess–paleosol sequences indicate oxidative transformation from eolian magnetite and authigenic magnetite to maghemite during pedogenesis.

In general, the extracted magnetic grains from loess units (e.g., L1 unit) are larger than those from paleosol units (e.g., S1 unit). Based on observations from TEM, optical microscope and XRD analyses, it is suggested that sub-micrometer magnetite grains were oxidized mainly into maghemite (Figs. 4 and 6) or magnetite–maghemite complexes (Figs. 5 and 8). Although powder XRD patterns show small amounts of hematite in the extracted magnetic samples (Figs. 2 and 3), reddish hematite coatings (or rims) only occur in coarse magnetite grains according to optical microscopic observation. Very fine grains and nano-crystals of magnetite were mainly transformed into maghemite, even though hematite is thermodynamically more stable than maghemite. It is proposed that decreasing the crystal size of maghemite or increasing its surface area may increase its stability. Magnetite nano-crystals could be transformed into maghemite completely. Oxidation products of magnetite at room temperature could be either maghemite or hematite, depending on original grain sizes of magnetite crystals. Of course, the size of the magnetite also affects its transformation rate. Synthetic experiments on magnetite oxidation show that its oxidation products could be dominated by maghemite or hematite depending on magnetite crystal sizes and impurities in the magnetite [40–42]. Small magnetite grains (less than ~1 μm) will favor maghemite formation during solid-state oxidative transformation [40–42].

Some magnetic grains show euhedral maghemite nanocrystals with a narrow range of size distribution (Figs. 9 and 10). Such maghemite was originally magnetite from magnetotactic bacteria. They are biogenic magnetite according to criteria for identifying magnetosomes [4,43], although they are not arranged in chain-like shapes. This kind of maghemite is more common in the paleosol units than in loess units. Magnetosomes were found in the Chinese loess–paleosol sequences by Jia [12]. Such kind of maghemite was suggested as a source of superparamagnetic particles and as the main mechanism of magnetic susceptibility enhancement. Maher et al. also considered euhedral magnetite grains with size range of 20–50 nm as magnetosomes, but

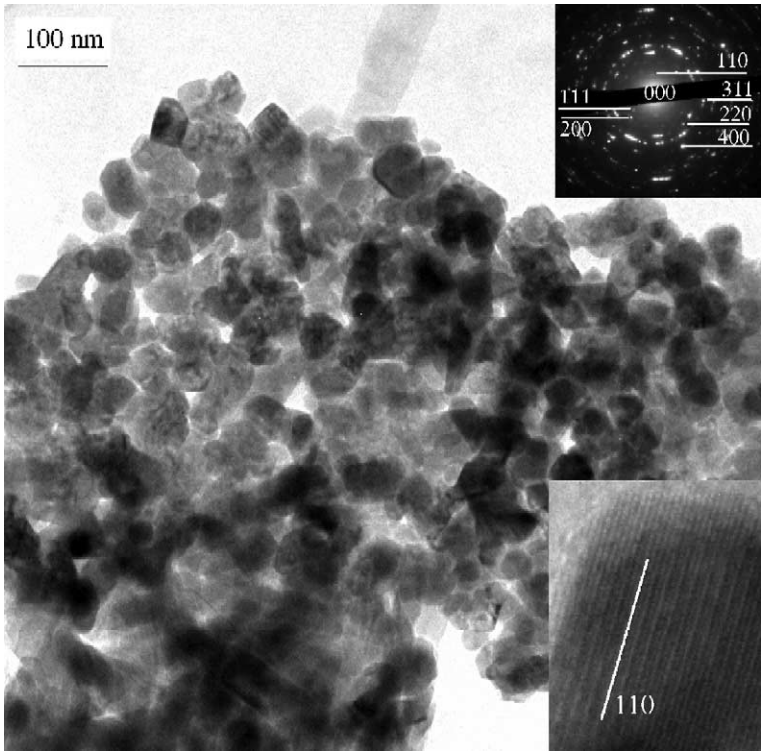

Fig. 9. TEM image inserted SAD (right upper corner) and lattice fringe (right down corner) shows narrow range of size distribution and euhedral maghemite crystals that were magnetite from magnetotactic bacteria or biogenic magnetite.

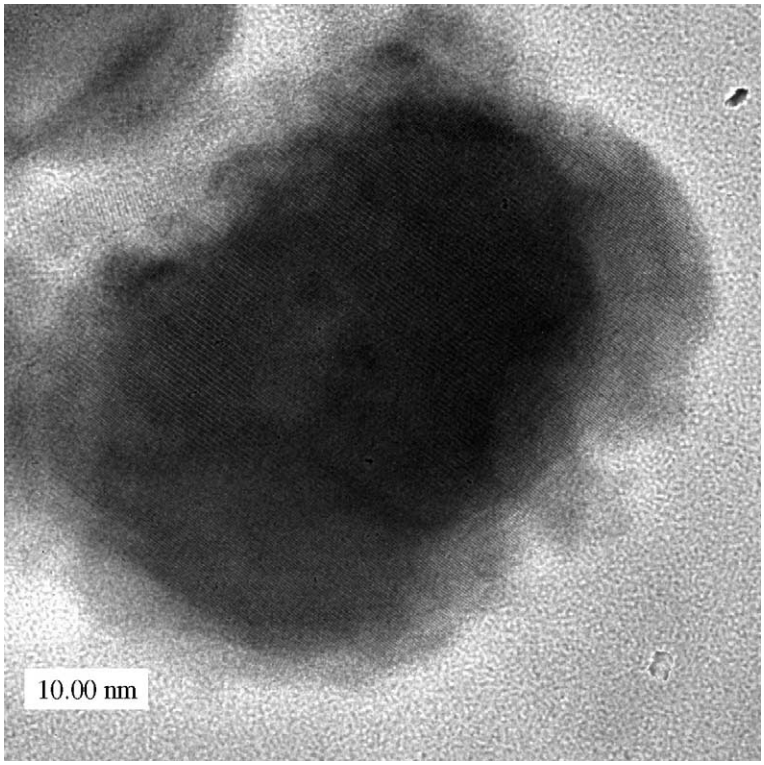

Fig. 10. HRTEM image shows a maghemite single crystal with (110) lattice fringes that was a magnetite grain from magnetotactic bacteria.

argued that they only play a secondary role in the magnetic susceptibility enhancement because of their small volume percentage in the loess–paleosol sequences [4,44,45]. The results of the TEM investigation indicate that all the magnetite nano-crystals similar to magnetosomes display (110) superstructure lattice fringe in maghemites (Fig. 10). Such kind of maghemite is directly related to microbial biomineralization. The maghemite nano-crystals were transformed from the oxidation of magnetosomes. Experimental study also confirms that nanometer-size magnetite can be easily oxidized into maghemites under room temperature condition [46].

Based on the above results, it can be inferred that the oxidation product of magnetite nano-crystals is maghemite at low temperature. Therefore, superparamagnetic particles in loess–paleosol sequences should be maghemite instead of magnetite. This result also confirms previous suggestions and magnetic property studies of the loess–paleosol sequences. It can be inferred that nanometer-scale maghemite is more stable than magnetite in the oxidizing environment. Maghemite nano-crystals may be more stable than hematite at room temperature in dry environments, although Diakonov suggested that maghemite will be stable with respect to hematite when the nano-crystals of maghemite reach surface areas of about 535 m^2/g [26]. McHale et al. [47] had found that γ-Al_2O_3 nano-crystal is more stable than α-Al_2O_3 nano-crystal because of the lower surface energy of γ-Al_2O_3 with respect to that of α-Al_2O_3. The structure of γ-Fe_2O_3 is same as that of γ-Al_2O_3, and so is the structure of α-Fe_2O_3. In a similar way, the surface energy of γ-Fe_2O_3 should be lower than that of α-Fe_2O_3 [48]. As a result, decreasing the crystal size of maghemite will increase its stability at room temperature.

Because maghemite was formed from low-temperature oxidation of magnetite, maghemite concentration in loess–paleosol sequences relates to the concentration of magnetite formed during pedogensis and grain size of eolian magnetite. Both magnetite magnetosomes and precipitated magnetite with nanoporous texture induced by iron-reducing bacteria are related to microbial activity in the soil environment. The size distribution of eolian origin magnetite grains is related to the intensity of the winter monsoon winds. Therefore, the concentration of authigenic magnetite, the weathering of the eolian magnetite, and the concentration of maghemite can be used as signatures of paleoclimate changes. Deng et al. [20] also suggested that strong pedogenesis will result in the high concentration and intense oxidation of magnetite.

5. Mechanism for the magnetic susceptibility enhancement

Maher [49] pointed out that the susceptibility of magnetite with crystal size of ~10 nm will be about four times higher than that with crystal sizes of several micrometers. The critical size for maghemite to be superparamagnetic is about 30–50 nm [46]. Our TEM results show that there are nanoporous maghemite grains composed of maghemite nano-crystals in paleosol samples (Fig. 6). Such kind of maghemite is directly related to microbial activity during pedogenesis. Our TEM results also provide the microstructural evidence for chemical weathering from magnetite to maghemite. Submicrometer-size eolian magnetite can be transformed into nanometer maghemite in the pedogenic process (Fig. 8), which changes ferromagnetic grains into superparamagnetic nano-crystals. We propose that maghemite has similar size-dependent magnetic susceptibility, although there is no reported data showing the relationship between magnetic susceptibility and its crystal sizes. It can be inferred that although the total amount of ferromagnetic particles (weight percentage) in paleosol units does not show an obvious increase with respect to that in loess units, magnetic susceptibility can be enhanced several times because of the formation of nano-crystalline maghemite.

It should be pointed out that although the overall particle size of the nanoporous maghemite is about micrometer or sub-micrometer scale, the crystalline domains are at the scale of ten or several tens of nanometers. The nano-crystal domains in weathered magnetite also enhance magnetic susceptibility. This process is related to chemical weathering. However, the role of microbes and bio-organics play an important role. This phenomenon may result in a disagreement between the crystal size of magnetic carriers in magnetism analyses and selected grain sizes for magnetic susceptibility analyses. The magnetic property study of loess samples suggests that magnetic susceptibility enhancement in paleosols results from authigenic fine-grained magnetite crystals (that has transformed to maghemite). However, Han et al. [50] argued that the content of nanometer-scale grains in loess–paleosol sequences is very small and its contribution to magnetic susceptibility is less than 5% according to susceptibility analyses from different grain size fractions of typical loess and paleosol units. Contributions to magnetic susceptibility are mainly from larger than 1-μm fraction grains in loess sample, because the loess unit contains more coarse grains (Fig. 11). Fig. 11A shows that there is no obvious change in magnetic susceptibility for

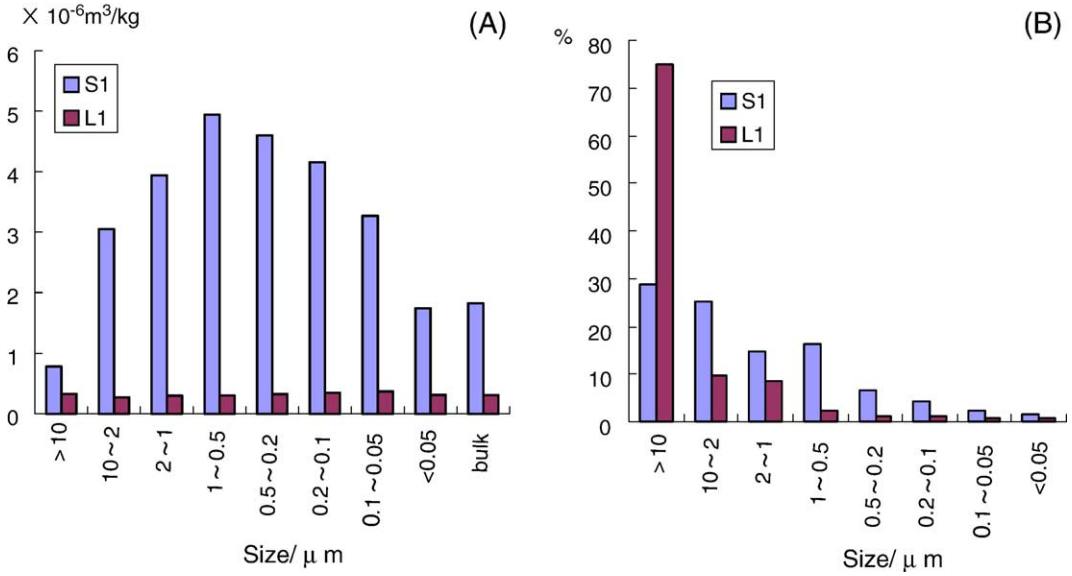

Fig. 11. Contribution of different size fractions to magnetic susceptibility and magnetic susceptibility of different size fraction samples from Xifeng section (calculated from the data in [50]). (A) Magnetic susceptibility of different size fractions; (B) contribution of different grain size fractions to magnetic susceptibility.

various fractions of the loess sample. However, the magnetic susceptibility for 1-μm and less than 1-μm fraction samples from paleosol sample increases significantly with respect to the loess sample, which indicates magnetic susceptibility enhancement in these size fractions. Han et al. suggested that magnetic susceptibility enhancement should be related to iron oxide evolution during pedogenesis but could not provide a detailed explanation for these processes. Our TEM results showing nano-crystalline maghemite explain the enhancement of the magnetic susceptibility in fine-grained fractions because of the formation of maghemite nano-crystals.

Recently, many authors have proposed the effect of microstructure and crystal size on their magnetic susceptibility anomalies. Harrison et al. [51] directly mapped the nanometer magnetic structure with electron holograms in TEM and gave an excellent explanation for the magnetic anomaly in their nano-structured magnet. McEnroe et al. [52] also found that the mechanism explaining the magnetic anomaly in massive ilmenite rock was the formation of nanometer-scale lamella of hematite and ilmenite during the exsolution of hematite–ilmenite solid solution. Brown and O'Reilly [42] found that magnetic susceptibility enhancement of pulverized natural titanomagnetite is related to nano-structure resulting from stress during ball-milling. Banfield et al. [23] proposed a connection between intergrown structure of massive magnetite–maghemite at the nano-meter scale and its strong magnetic property. All the previous results indicate that nano-structures of magnetic grains may cause magnetic susceptibility enhancement for magnetite and maghemite.

6. Conclusions

Based on our direct observations in TEM and XRD studies, it can be concluded that sub-micrometer- and nanometer-size magnetites were completely oxidized into maghemite during the pedogenic (soil formation) process. The oxidized products of sub-micrometer magnetite have multi-domain structure that is composed of maghemite nano-crystals. Biogenetic magnetite can be preserved as maghemite in loess–paleosol sequences that formed during solid-state transformation from magnetite to maghemite. Some nano-crystalline maghemites with nanoporous texture resulted from microbe-induced precipitation of magnetite or transformation of poorly crystalline ferric Fe (oxy)hydroxides by Fe-reducing bacteria. The crystal size of maghemite will affect its stability. Maghemite with small size (~ nanometer scale) is more stable than that with large size. Superparamagnetic particles composed of maghemite nano-crystals are the main carrier of magnetic susceptibility in the loess and paleosols. We suggest the formation of nano-structured maghemite and biogenic magnetite are responsible for the magnetic susceptibility enhancement in the paleosol units. HRTEM with associated analytical techniques is a useful tool for

studying mechanisms for the magnetic susceptibility enhancement in paleosols.

Acknowledgement

The work was supported by the National Natural Science Foundation of China (40331001, 40472026), the Outstanding Overseas Chinese Scholars Fund of the Chinese Academy of Sciences (2003-1-7), and the National Science Foundation (EAR02-0210820). The authors thank the Department of Geology and Geophysics of the University of Wisconsin for partial support of this study. The authors also thank Joe Mason, Ed Boyle, and an anonymous reviewer for providing helpful comments and suggestions.

References

[1] G. Kukla, Z.S. An, Loess stratigraphy in central China, Palaeogeogr. Palaeoclimatol. Palaeoecol. 72 (1989) 203–225.
[2] X.M. Liu, T. Rolph, J. Bloemendal, J. Shaw, T.S. Liu, Quantitative estimates of palaeoprecipitation at Xifeng, in the loess plateau of China, Palaeogeogr. Palaeoclimatol. Palaeoecol. 113 (1995) 243–248.
[3] B.A. Maher, A. Alekseev, T. Alekseeva, Variation of soil magnetism across the Russian steppe: its significance for use of soil magnetism as a palaeorainfall proxy, Quat. Sci. Rev. 21 (2002) 1571–1576.
[4] B.A. Maher, R. Thompson, Paleorainfall reconstructions from pedogenic magnetic susceptibility variations in the Chinese loess and paleosols, Quat. Res. 44 (1995) 383–391.
[5] F. Heller, C.D. Shen, J. Beer, X.M. Liu, T.S. Liu, A. Bronger, M. Suter, G. Bonani, Quantitative estimates of pedogenic ferromagnetic mineral formation in Chinese loess and palaeoclimatic implications, Earth Planet. Sci. Lett. 114 (1993) 385–390.
[6] H.Y. Lu, J.M. Han, N.Q. Wu, Magnetic susceptibility of modern soil and its palaeoclimate implications, Sci. China (series D) 24 (12) (1994) 1290–1297.
[7] F. Heler, T.S. Liu, Paleoclimatic and sedimentary history from magnetic susceptibility of loess in China, Geophys. Res. Lett. 13 (1986) 1169–1172.
[8] G. Kukla, F. Heller, X. Liu, T.C. Xu, T.S. Liu, Z.S. An, Pleistocene climates dated by magnetic susceptibility, Geology 16 (1988) 811–814.
[9] G. Kleteschka, S.K. Banerjee, Magnetic stratigraphy of Chinese loess as a record of natural fire, Geophys. Res. Lett. 22 (1995) 1341–1343.
[10] H. Zheng, F. Oldfield, L. Yu, J. Shaw, Z.S. An, The magnetic properties of particle-sized samples from the Luo Chuan loess section: evidence for pedogenesis, Phys. Earth Planet. Int. 68 (1991) 250–258.
[11] L.P. Zhou, F. Oldfield, A.G. Wintle, S.G. Robinson, J.T. Wang, Partly pedogenic origin of magnetic variations in Chinese loess, Nature 346 (1990) 737–739.
[12] R.F. Jia, B.Z. Yan, R.S. Li, Characteristics of magnetosome bacterias of loess samples from Duanjiapo profile in Shanxi province and palaeoclimate implications, Sci. China(Series D) 26 (1996) 411–416.
[13] F. Heller, T.S. Liu, Magnetism of Chinese loess deposits, Geophys. J. Roy. Astron. Soc. 77 (1984) 125–141.
[14] J.F. Ji, J. Chen, L. Jin, W.C. Zhang, W. Balsam, H.Y. Lu, Relating magnetic susceptibility (MS) to the simulated thematic mapper (TM) bands of the Chinese loess: application of TM image for soil MS mapping on Loess Plateau, J. Geophys. Res. 109 (2004) 5102–5112.
[15] K.L. Verosub, P. Fine, M.J. Singer, J. Tenpas, Pedogenesis and paleoclimate: interpretation of the magnetic susceptibility record of Chinese loess–paleosol sequences, Geology 21 (1993) 1011–1014.
[16] J.K. Eyre, J. Shaw, Magnetic enhancement of Chinese loess—the role of γ-Fe_2O_3? Geophys. J. Int. 117 (1994) 265–271.
[17] C.P. Hunt, S.K. Banerjee, J.M. Han, P.A. Solheid, E. Oches, W.W. Sun, T.S. Liu, Rock-magnetic proxies of climate change in the loess–palaeosol sequence of the western Loess Plateau of China, Geophys. J. Int. 123 (1995) 232–244.
[18] W.W. Sun, S.K. Banerjee, C.P. Hunt, The role of maghemite in the enchancement of magnetic signal in the Chinese loess–paleosol sequence: an extensive rock magnetic study combined with citrate–bicarbnonate–dithionite treatment, Earth Planet. Sci. Lett. 133 (1995) 493–505.
[19] X.M. Liu, P. Hesse, T. Rolph T, Origin of maghaemite in Chinese loess deposits: aeolian or pedogenic? Phys. Earth Planet. Int. 112 (1999) 191–201.
[20] C.L. Deng, R.X. Zhu, M.J. Jackson, Variability of the temperature-dependent susceptibility of the Holocene eolian deposits in the Chinese loess plateau: a pedogenesis indicator, Phys. Chem. Earth, Part A Solid Earth Geo. 26 (2001) 873–878.
[21] R.E. Vandenberghe, J.J. Hus, D.E. Grave, Evidence from Mossbauer spectroscopy of neo-formation of magnetite/maghemite in the soils of loess/paleosol sequence in China, Hyper. Int. 117 (1998) 359–369.
[22] S. Glasauer, S. Langley, T.J. Beveridge, Intracellular iron minerals in a dissimilatory iron-reducing bacterium, Science 295 (2002) 117–119.
[23] J.F. Banfield, P.J. Wasilewski, D.R. Veblen, TEM study of relationships between the microstructures and magnetic properties of strongly magnetized magnetite and maghemite, Am. Miner. 79 (1994) 654–667.
[24] J. Tang, M. Myers, K.A. Bosnick, L.E. Brus, Magnetite Fe_3O_4 nanocrystals: spectroscopic observation of aqueous oxidation kinetics, J. Phys. Chem. 107 (2003) 7501–7506.
[25] J.J. Hus, B. Bater, Magnetic hysteresis parameters of bulk samples and particle-size fractions of the loess/palaeosol sequence in Central China, Geol. Carpath. 44 (1993) 325–333.
[26] I. Diakonov, Thermodynamic properties of iron oxides and hydroxides: II. Estimation of the surface and bulk thermodynamic properties of ordered and disordered maghemite (γ-Fe_2O_3), Eur. J. Miner. 10 (1988) 17–29.
[27] P.R. Buseck, Minerals and reactions at the atomic scale: transmission electron microscopy, Rev. Mineral. 27 (1992) 1–508.
[28] M.F. Hochella, J.N. Moore, U. Golla, A. Putnis, A TEM study of samples from acid mine drainage systems: metal–mineral association with implications for transport, Geochim. Cosmochim. Acta 63 (1999) 3395–3406.
[29] D.E. Janney, J.M. Cowley, P.T. Buseck, Structure of synthetic 6-line ferryhydrite by electron nanodiffraction, Am. Miner. 86 (2001) 327–335.
[30] J.F. Banfield, S.A. Welch, H.Z. Zhang, T.T. Ebert, R.L. Penn, Aggregation-based crystal growth and microstructure develop-

ment in natural iron oxyhydroxide biomineralization products, Science 289 (2000) 751–754.
[31] T.H. Chen, H.F. Xu, J.F. Ji, J. Chen J, Y. Chen, Formation mechanism of ferromagnetic minerals in Loess of China: TEM investigation, Chin. Sci. Bull. 48 (2003) 2259–2266.
[32] M.W. Hounslow, B.A. Maher, Laboratory procedures for quantitative extraction and analysis of magnetic minerals from sediments, in: J. Walden, F. Oldfield, J.P. Smith (Eds.), Environmental Magnetism: A Practical Guide, Extraction and Analysis of Magnetic Minerals from Sediments, Quaternary Research Association, Cambridge, UK, 1999, pp. 139–184.
[33] H.F. Xu, Y.F. Wang, Crystallization sequence and microstructure evolution of Synroc samples crystallized from $CaZrTi_2O_7$ melts, J. Nucl. Mater. 279 (2000) 100–106.
[34] H.F. Xu, Y.F. Wang, Electron energy-loss spectroscopy (EELS) study of oxidation states of Ce and U in pyrochlore and uraninite—natural analogues for Pu- and U-bearing waste forms, J. Nucl. Mater. 265 (1999) 117–123.
[35] L.A.J. Garvie, A.J. Craenv, Use of electron-energy loss near-edge fine structure in the study of minerals, Am. Miner. 79 (1994) 411–425.
[36] G.A. Waychunas, Crystal chemistry of oxides and oxyhydroxides, Rev. Miner. 25 (1991) 11–68.
[37] H.F. Xu, Using electron energy-loss spectroscopy associated with transmission electron microscopy to determine oxidation states of Ce and Fe in minerals, Geol. J. China Univ. 6 (2000) 137–144.
[38] R. Cornell, U. Schwertmann, The iron oxide: structure, properties, reactions, occurrence, and use, VCH Verlagsgesellschaft, Weinheim, 1996, 573 pp.
[39] K.L. Grogan, R.J. Gilkes, B.G Lottermoser, Maghemite formation in burnt plant litter at East Trinity, North Queensland, Australia, Clays Clay Miner. 51 (2003) 390–396.
[40] K.J. Gallagher, W. Feitknecht, U. Mannweiler, Mechanism of oxidation of magnetite to γ-Fe_2O_3, Nature 217 (1968) 1118–1119.
[41] U. Colombo, F. Gazzarrini, G. Lanzavercchia, G. Sironi, Magnetite oxidation: a proposed mechanism, Science 147 (1965) 1033.
[42] A.P. Brown, W. O'Reilly, The magnetism and microstructure of pulverized titanomagnetite, $Fe_{2.4}Ti_{0.6}O_4$: the effect of annealing, maghemitization and inversion, Phys. Earth Planet. Int. 116 (1999) 19–30.
[43] B. Devouard, M. Posfai, X. Hua, D.A. Bazylinski, R.B. Frankel, P.R. Buseck, Magnetite from magnetotactic bacteria: size distributions and twinning, Am. Miner. 83 (1998) 1387–1398.
[44] B.A. Maher, R. Thompson, Paleoclimatic significance of the mineral magnetic record of the Chinese loess and paleosols, Quat. Res. 37 (1992) 155–170.
[45] B.A. Maher, R. Thompson, L.P. Zhou, Spatial and temporal reconstructions of changes in the Asian palaeomonsoon: a new mineral magnetic approach, Earth Planet. Sci. Lett. 125 (1994) 461–471.
[46] Y.W. Dou, H.L. Luo, Magnetic Record Materials, Electron Technology Publish, Beijing, 1992, (in Chinese) 206 pp.
[47] J.M. McHale, A. Auroux, A.J. Perrotta, A. Navrotsky, Surface energies and thermodynamic phase stability in nanocrystalline aluminas, Science 277 (1997) 788–791.
[48] G. Schimanke, M. Martin, In situ XRD study of the phase transition of nanocrytalline maghemite (γ-Fe_2O_3) to hematite (α-Fe_2O_3), Soilid State Ion. 136–137 (2000) 1235–1240.
[49] B.A. Maher, Magnetic properties of some synthetic sub-micron magnetites, Geophys. J. Int. 94 (1988) 83–96.
[50] J.M. Han, W.Y. Jiang, J. Chu J, Grain size distribution of magnetic minerals in loess and paleosol, Quat. Sci. 281–287 (1997) (in Chinese).
[51] R.J. Harrison, R.E. Dunin-Borkowski, A. Putnis, Direct imaging of nanoscale magnetic interactions in minerals, Prog. Natl. Acad. Sci. U. S. A. 99 (2002) 16556–16561.
[52] S.A. McEnroe, R.J. Harrison, P. Robinson, F. Langenhorst, Nanoscale haematite–ilmenite lamellae in massive ilmenite rock: an example of 'lamellar magnetism' with implications for planetary magnetic anomalies, Geophys. J. Int. 151 (2002) 890–912.
[53] P. Braun, A superstructure in spinels, Nature 170 (1952) 1123.
[54] P.P.K. Smith, The observation of enantiomorphous domains in a natural maghemite, Contrib. Mineral. Petrol. 69 (1979) 249–254.
[55] C. Greaves, A powder neutron diffraction investigation of vacancy and covalence in γ-ferric oxide, J. Solid State Chem. 30 (1983) 257–263.
[56] D.R. Lovley, Dissimilatory Fe(III) and Mn(IV) reduction, Microbiol. Rev. 55 (1991) 259–287.
[57] D.R. Lovley, Fe(III) and Mn(IV) reduction, in: D.R. Lovley (Ed.), Environmental Metal-Microbe Interactions, ASM Press, Washington, DC, 2000, pp. 3–30.
[58] C.M. Johnson, E.E. Roden, S.A. Welch, B.L. Beard, Experimental constraints on Fe isotope fractionation during magnetite and Fe carbonate formation coupled to dissimilatory hydrous ferric oxide reduction, Geochim. Cosmochim. Acta 69 (2005) 963–993.
[59] E.E. Roden, Fe (III) oxide reactivity toward biological versus chemical reduction, Environ. Sci. Technol. 37 (2003) 1319–1324.